NUCLEAR THEORY, Vol. 42 (2025)
eds. M. Gaidarov, N. Minkov, Heron Press, Sofia

Giant Monopole Resonance Excitation Energy: Systematic Analysis and Open Problems

M.K. Gaidarov[1,2], **M.V. Ivanov**[1,2], **Y.I. Katsarov**[1], **A.N. Antonov**[1], **I.C. Danchev**[3]

[1]Institute for Nuclear Research and Nuclear Energy, Bulgarian Academy of Sciences, Sofia 1784, Bulgaria

[2]Department of Mathematics and Physics, Faculty of Mathematics and Natural Sciences, Neofit Rilski South-West University, Blagoevgrad, Bulgaria

[3]Department of Physical and Mathematical Sciences, School of Arts and Sciences, University of Mount Olive, 652 R.B. Butler Dr., Mount Olive, NC 28365, USA

Abstract. Results for the isoscalar giant monopole resonance (ISGMR) in a wide range of nuclei from various isotopic chains are presented. They are obtained within the microscopic self-consistent Skyrme HF+BCS method and the coherent density fluctuation model. Different definitions of the ISGMR energy are applied and two energy-density functionals for nuclear matter are used to calculate the nuclear incompressibility: Brueckner and Barcelona-Catania-Paris-Madrid. The problems related to the lack of precise data for the neutron (and matter) rms radii in the analysis of the ISGMR energy are pointed out and discussed. A connection with the measured neutron skin thicknesses is proposed as a possible way for realistic estimations of the ISGMR centroid energy.

1 Introduction

The giant resonances are clear manifestation of the nuclear collective motion. Particularly, the isoscalar giant monopole resonance (ISGMR) measures the collective response of the nucleus to density fluctuations. The energy of this resonance is closely related to the incompressibility of the nucleus, which, in turn, can be linked to the incompressibility of the infinite nuclear matter, which is an important ingredient of the nuclear matter equation of state (EOS).

An important primary motivation for studying the ISGMR is to probe bulk nuclear properties of the nuclear EOS. As such, it is highly unexpected that effects arising from microscopic shell structure would appreciably influence the collective behavior of the nucleus undergoing these excitations. The isoscalar resonances are excited through low-momentum transfer reactions in inverse kinematics, which require special detection devices. At present, promising results have been obtained using active targets. Different measurements have been conducted on Ni isotopes far from stability, namely ^{56}Ni [1, 2] and ^{68}Ni [3, 4]. In particular, the experiment with ^{68}Ni is the first measurement of the isoscalar

monopole response in a short-lived neutron-rich nucleus using inelastic alpha scattering. The ISGMR was found to be fragmented, with a possible indication for the soft monopole resonance.

A first attempt to study the ISGMR in Ni, Sn, and Pb isotopes within the microscopic self-consistent Skyrme HF+BCS method and CDFM was performed in our previous work [5]. The obtained results of calculations based on the Brueckner energy-density functional (EDF) for nuclear matter have demonstrated the relevance of the proposed theoretical approach to probe the excitation energy of the ISGMR in various nuclei. In the present work (as well as in Ref. [6]), the incompressibility and the centroid energy of ISGMR are studied in a wide range of finite nuclei using an extended method on the basis of the Brueckner [7, 8] as well as BCPM [9–11] functionals for nuclear matter and the coherent density fluctuation model (CDFM) (e.g., Refs. [12,13]). The latter is a natural extension of the Fermi gas model based on the generator coordinate method [13, 14] and includes long-range correlations of collective type. The results for the excitation energies of ISGMR are obtained by using its two definitions given in literature. Complimentary to the consideration in Ref. [5], in this work a variety of different even-even nuclei from ^{40}Ca to ^{208}Pb is considered and results for the energy of the ISGMR are presented and discussed in comparison with the experimental data. In addition, we analyze the values of the centroid energies of Sn isotopes (A=112-124), as well as ^{48}Ca and ^{208}Pb nuclei, studying their isotopic sensitivity by adding results on the base of experimentally measured neutron skin thickness.

2 Theoretical Formalism

Based on the relationships used to obtain the energy of the ISGMR through the incompressibility K^A of a nucleus with Z protons and N neutrons, there are two definitions which will be used further in our calculations. One of them is (see Ref. [15])

$$E_{ISGMR} = \frac{\hbar}{r_0 A^{1/3}} \sqrt{\frac{K^A}{m}}, \tag{1}$$

where $A = Z + N$ is the mass number, m is the nucleon mass and r_0 is a radius parameter deduced from the equilibrium density.

The second definition is given in the scaling method [16] as

$$E_{ISGMR} = \hbar \sqrt{\frac{K^A}{m < r^2 >}}, \tag{2}$$

where $< r^2 >$ is the mean square mass radius of the nucleus in the ground state. We note that Eq. (2) does not contain a fit parameter and directly uses the radii obtained from mean-field calculations.

The mean square radii for protons and neutrons are obtained using the corresponding definitions:

$$< r^2_{p,n} >= \frac{\int r^2 \rho_{p,n}(\mathbf{r}) d\mathbf{r}}{\int \rho_{p,n}(\mathbf{r}) d\mathbf{r}}, \tag{3}$$

while the matter mean square radius $< r^2 >$ entering Eq. (2) can be calculated by the expression:

$$< r^2 >= \frac{N}{A} < r^2_n > + \frac{Z}{A} < r^2_p > . \tag{4}$$

The expressions for the single-particle wave functions and densities $\rho_{p,n}(r)$ obtained within the self-consistent deformed Hartree-Fock method with density-dependent SLy4 interaction and pairing correlations are given, e.g., in Ref. [17].

Within the CDFM the one-body density matrix (OBDM) $\rho(\mathbf{r}, \mathbf{r}')$ of the nucleus is a superposition of OBDM's $\rho_x(\mathbf{r}, \mathbf{r}')$ of spherical "pieces" of nuclear matter (called "fluctons") with radius x in which all A nucleons are uniformly distributed:

$$\rho(\mathbf{r}, \mathbf{r}') = \int_0^\infty dx |F(x)|^2 \rho_x(\mathbf{r}, \mathbf{r}') \tag{5}$$

with

$$\rho_x(\mathbf{r}, \mathbf{r}') = 3\rho_0(x) \frac{j_1(k_F(x)|\mathbf{r} - \mathbf{r}'|)}{(k_F(x)|\mathbf{r} - \mathbf{r}'|)} \Theta\left(x - \frac{|\mathbf{r} + \mathbf{r}'|}{2}\right). \tag{6}$$

In Eq. (6)

$$\rho_0(x) = \frac{3A}{4\pi x^3}, \tag{7}$$

$$k_F(x) = \left(\frac{3\pi^2}{2}\rho_0(x)\right)^{1/3} \equiv \frac{\alpha}{x} \tag{8}$$

with

$$\alpha = \left(\frac{9\pi A}{8}\right)^{1/3} \simeq 1.52 A^{1/3}, \tag{9}$$

Θ is the step-function of Heaviside, and j_1 is the first-order spherical Bessel function. The nucleon density distribution is given by the diagonal elements of the OBDM (5):

$$\rho(\mathbf{r}) = \rho(\mathbf{r}, \mathbf{r}) = \int_0^\infty dx |F(x)|^2 \rho_0(x) \Theta(x - |\mathbf{r}|). \tag{10}$$

It can be seen from Eq. (10) that in the case of monotonically decreasing local density ($d\rho/dr \leq 0$) the weight function $|F(x)|^2$ in CDFM (normalized to unity) can be obtained:

$$|F(x)|^2 = -\frac{1}{\rho_0(x)} \left.\frac{d\rho(r)}{dr}\right|_{r=x}. \tag{11}$$

In the CDFM scheme, the symmetry energy of finite nuclei has the form:

$$S^A = \int_0^\infty dx|F(x)|^2 S(\rho_0(x)). \tag{12}$$

Similarly, the incompressibility in finite nuclei K^A is written in the form

$$K^A = \int_0^\infty dx|F(x)|^2 K(\rho_0(x)). \tag{13}$$

In Eqs. (12) and (13) the weight function $|F(x)|^2$ is given by Eq. (11). The functions $S(\rho_0(x))$ and $K(\rho_0(x))$ in the integrand of both equations are correspondingly the symmetry energy and the incompressibility in infinite nuclear matter. A detailed information about the method how to obtain the intrinsic quantity K^A can be found in Ref. [6].

Next, we give the expressions for the EDFs used in the present work. We consider the energy as a sum of the kinetic $T(\rho,\alpha)$ and the potential $V(\rho,\alpha)$ contributions

$$\frac{E(\rho,\alpha)}{A} = T(\rho,\alpha) + V(\rho,\alpha), \quad \alpha = \frac{N-Z}{A} \tag{14}$$

in both approaches for EDF, namely that one of Brueckner [7, 8] and of the Barcelona-Catania-Paris-Madrid (BCPM) one (see, e.g. Ref. [9–11] and references therein).

The kinetic energy part of the EDF used is of the Thomas–Fermi type:

$$T(\rho,\alpha) = \frac{C}{2}[(1+\alpha)^{5/3} + (1-\alpha)^{5/3}]\rho^{2/3}. \tag{15}$$

We use two types of the potential part of the EDF $V(\rho,\alpha)$:

i) That one from the Brueckner EDF [8]:

$$V(\rho,\alpha) = b_1\rho + b_2\rho^{4/3} + b_3\rho^{5/3} + \alpha^2(b_4\rho + b_5\rho^{4/3} + b_6\rho^{5/3}) \tag{16}$$

and

ii) The potential part of the BCPM [further called BCPM(v)] EDF (see, e.g., Ref. [9]):

$$V(\rho,\alpha) = \sum_{n=1}^{5} a_n \Big(\frac{\rho}{\rho_\infty}\Big)^n (1-\alpha^2) + \sum_{n=1}^{5} b_n \Big(\frac{\rho}{\rho_{0n}}\Big)^n \alpha^2. \tag{17}$$

The values of the parameters in Eqs. (16) and (17) are listed in the Appendix of Ref. [6].

3 Results and Discussion

We start our analysis by showing in Table 1 the values of the incompressibility K^A and the corresponding energy E_{ISGMR} calculated in the present work using Eq. (2). The latter are compared with the available experimental data for the same range of nuclei including Ca, Fe, Ni, and Pb isotopes. We should mention that the results for the centroid energy in the case of the Brueckner EDF are in good agreement with the data for isotopes of Ca, Fe, and Ni. In the case of BCMP(v) EDF they are comparable in the case of ^{68}Ni and partly for some isotopes of Pb.

Concerning the use of Eq. (2), in particular the nuclear root-mean-square (rms) radii in it, we would like to note the following: i) the rms radii can be calculated on the base of experimentally obtained proton density distributions by means of electromagnetic interaction and some other processes; ii) while in many cases the charge densities are well known (see, e.g., Ref. [18]) with relatively high accuracy, this is not the case with the neutron densities which could not be precisely obtained due to the charge neutrality of the neutrons.

Table 1. The values of K^A and E_{ISGMR} calculated using Brueckner and BCPM(v) EDFs and Eq. (2), along with rms radii and experimental data for the ISGMR energy

	Brueckner		BCPM(v)			
Nuclei	K^A [MeV]	E_{ISGMR} [MeV]	K^A [MeV]	E_{ISGMR} [MeV]	$\langle r^2\rangle^{1/2}$ [fm]	Exp. [MeV]
^{40}Ca	108.53	19.76	172.53	24.92	3.40	19.18 ± 0.37
^{42}Ca	109.98	19.67	175.47	24.85	3.43	19.7 ± 0.1
^{44}Ca	109.94	19.45	177.14	24.69	3.47	19.49 ± 0.34
^{46}Ca	108.54	19.12	176.02	24.35	3.51	
^{48}Ca	107.08	18.81	176.99	24.18	3.54	19.88 ± 0.16
^{54}Fe	117.90	19.20	186.83	24.17	3.64	19.66 ± 0.37
^{56}Ni	118.91	19.12	188.24	24.05	3.67	19.1 ± 0.5
^{58}Ni	117.42	18.78	186.78	23.69	3.72	18.43 ± 0.15
^{60}Ni	115.47	18.42	185.05	23.32	3.76	17.62 ± 0.15
^{68}Ni	105.43	16.80	176.58	21.74	3.94	21.1 ± 1.9
^{204}Pb	97.31	11.50	166.26	15.03	5.53	13.98
^{206}Pb	96.55	11.42	166.31	14.99	5.54	13.94
^{208}Pb	95.67	11.34	165.85	14.93	5.56	13.96 ± 0.2

Our next step is to consider the rare cases, where data extracted for the neutron skin thickness with probes having different sensitivities to the proton and neutron distributions are available. As an example, we analyze the Sn isotopic chain ($A = 112 - 124$). Usually the neutron skin thickness in heavy nuclei is defined as

$$\Delta r_{np} = < r_n^2 >^{1/2} - < r_p^2 >^{1/2} . \tag{18}$$

The "semi-empirical" procedure aims to determine the mean square mass radius $< r^2 >$ entering Eq. (2) starting from the experimental values of Δr_{np}. They are measured in different methods and shown in Fig. 4 of Ref. [19]. As known, a measurement of the neutron density distributions to a precision and detail comparable to that of the proton one is hardly possible. Having the proton rms radii calculated from the charge radii determined with a high accuracy [18, 20], the neutron rms radii can be obtained from Eq. (18). Then, the matter mean square radius $< r^2 >$ are calculated using Eq. (4). The resulting centroid energies E_{ISGMR} calculated using Eq. (2) are displayed in Figure 1. In the same figure a comparison with the available experimental data [21] is made. Both Brueckner and BCPM(v) functionals provide excitation energies whose values almost coincide with the calculated ones given in Table 1. The small differences in the excitation energy values represent a clear indication of the minimal role of the radius calculated from the empirical data for the neutron skins in Sn isotopes. However, we would like to note the importance of such kind of "alternative" estimations (where possible) that avoid the ambiguities in determination of the neutron rms radii both experimentally and theoretically.

As additional examples of this procedure, we consider two more nuclei, ^{208}Pb and ^{48}Ca, for which the neutron skin thickness has been recently extracted from parity-violating experiments PREX-II [22] and CREX [23], respectively.

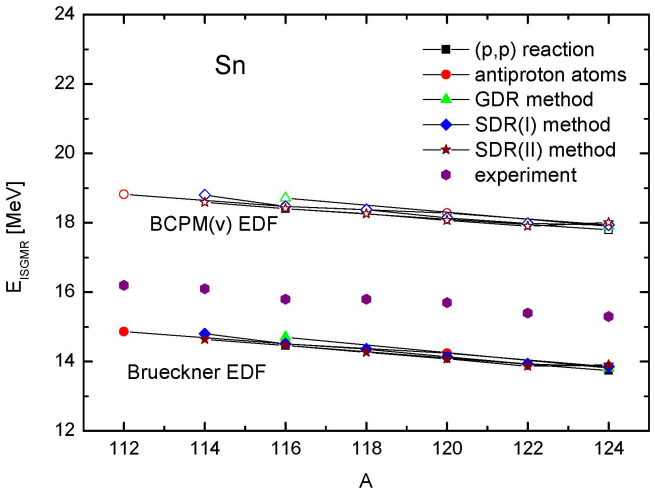

Figure 1. The centroid energies E_{ISGMR} as a function of the mass number A of Sn isotopes ($A = 112 - 124$) obtained with Brueckner (full symbols) and BCPM(v) (open symbols) EDFs by using the information for the neutron skin thickness extracted from various experiments including (p, p) scattering (squares), antiprotonic atoms (circle), the giant dipole resonance (GDR) method (triangles), and the spin-dipole resonance (SDR) method (diamonds and stars). The experimental data (hexagons) are taken from Ref. [21].

The relatively large neutron skin thickness $\Delta r_{np}(^{208}\text{Pb})=0.283 \pm 0.071$ fm extracted from PREX-II and the small value $\Delta r_{np}(^{48}\text{Ca})=0.121 \pm 0.026 \pm 0.024$ fm extracted from CREX are discussed in Ref. [24]. In this sense, we want to see the influence of the differences between PREX-II and CREX on the monopole excitations in ^{208}Pb and ^{48}Ca nuclei. The values of the rms radii deduced from the procedure are $< r^2 >^{1/2}(^{48}\text{Ca})=3.432$ fm and $< r^2 >^{1/2}(^{208}\text{Pb})=5.608$ fm, respectively, which are close to the calculated values listed in Table 1. For ^{48}Ca nucleus this leads to centroid energies E_{ISGMR} of 19.42 ± 0.170 MeV and 24.97 ± 0.170 MeV when applying Brueckner and BCPM(v) EDFs, while for ^{208}Pb the corresponding values are 11.24 ± 0.088 MeV and 14.80 ± 0.116 MeV. It can be seen that, taking into account the estimated error in the case of Brueckner EDF, the extracted value of the E_{ISGMR} for ^{48}Ca, using the neutron skin thickness reported by the CREX collaboration, fits well the experimental data.

The general question still stands, namely, which one, Eq. (1) or Eq. (2) to be used in the calculations of E_{ISGMR}. The point is that there are two different quantities related to the size of the nucleus in Eq. (1) and Eq. (2), namely, $r_0 A^{1/3}$ in Eq. (1) and the rms radius $< r^2 >^{1/2}$ in Eq. (2). For this purpose we give in what follows the results for E_{ISGMR} obtained from calculations using Eq. (1), where the nuclear radius is given by $R = r_0 A^{1/3}$, r_0 being a radial parameter of density distributions obtained from different experiments. Using the comparison of E_{ISGMR} with the experimental data, we performed a more detailed semi-empirical analysis of the parameter r_0. We parameterized it in a form:

$$r_0 = (1 + x/A^y) \tag{19}$$

and obtained values of x and y from the fit of E_{ISGMR} with the data for two nuclei in both limits of the considered nuclear range, namely for ^{40}Ca and ^{208}Pb. In the case of ^{40}Ca r_0=1.205 fm and in ^{208}Pb r_0=1.068 fm. These two conditions lead to the approximated values of x=2.40 fm and y=2/3. Thus, we obtained the following expression for the radius in the denominator of Eq. (1):

$$R = r_0 A^{1/3} = [1 + 2.40/A^{2/3}]A^{1/3}. \tag{20}$$

In our opinion, the second term in the right-hand side of Eq. (20) $2.40/A^{1/3}$ is related to the diffuse nuclear surface which changes its range from medium to heavy nuclei. The dependence of the radial parameter $r_0 = 1 + 2.40/A^{2/3}$ on the mass number between ^{40}Ca and ^{208}Pb is shown in Figure 2. The results of the calculations of E_{ISGMR} using Eqs. (1), (19) and (20) in both cases [with the EDFs of Brueckner and BCMP(v)] are listed in Table 2. It can be seen that in this case the results of E_{ISGMR} where the BCPM(v) method is used are in good agreement with the experimental data for almost all of the considered nuclei, which is not the case when the Brueckner EDF is used.

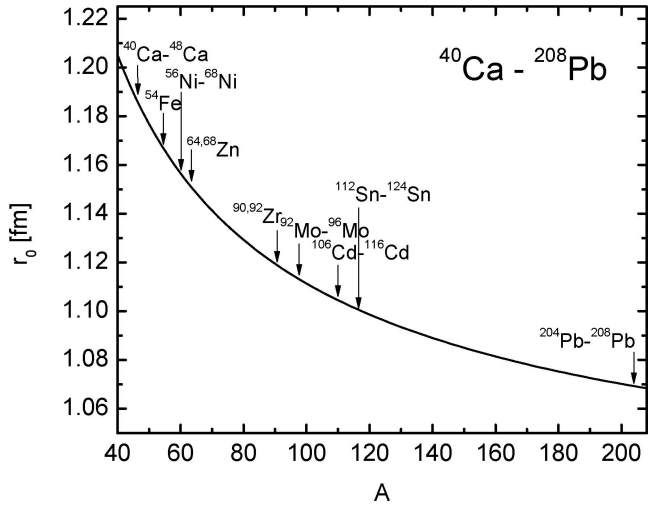

Figure 2. The dependence of the radius parameter r_0 (in fm) entering Eq. (1) on the mass number A for the considered nuclei between ^{40}Ca and ^{208}Pb.

Table 2. The values of E_{ISGMR} calculated using Brueckner and BCPM(v) density functionals and Eqs. (1), (19) and (20) and compared with the experimental data

Nuclei	r_0 [fm]	$r_0 A^{1/3}$ [fm]	$E_{ISGMR}^{\text{Brueckner}}$ [MeV]	$E_{ISGMR}^{BCPM(v)}$ [MeV]	Exp. [MeV]
^{90}Zr	1.120	5.02	13.57	17.14	16.9 ± 0.1
^{92}Zr	1.118	5.05	13.35	16.99	16.5 ± 0.1
^{92}Mo	1.118	5.05	13.57	17.10	16.6 ± 0.1
^{94}Mo	1.116	5.07	13.39	16.95	16.4 ± 0.2
^{96}Mo	1.114	5.10	13.18	16.77	16.3 ± 0.2
^{106}Cd	1.107	5.24	12.94	16.36	16.27 ± 0.09
^{110}Cd	1.105	5.29	12.67	16.11	15.94 ± 0.07
^{112}Cd	1.103	5.32	12.52	16.00	15.80 ± 0.05
^{114}Cd	1.102	5.34	12.38	15.87	15.61 ± 0.08
^{116}Cd	1.101	5.37	12.21	15.71	15.44 ± 0.06
^{112}Sn	1.103	5.32	12.72	16.11	16.2 ± 0.1
^{114}Sn	1.102	5.34	12.60	15.99	16.1 ± 0.1
^{116}Sn	1.101	5.37	12.45	15.85	15.8 ± 0.1
^{118}Sn	1.100	5.40	12.31	15.75	15.8 ± 0.1
^{120}Sn	1.099	5.42	12.18	15.64	15.7 ± 0.1
^{122}Sn	1.098	5.45	12.04	15.54	15.4 ± 0.1
^{124}Sn	1.097	5.47	11.91	15.43	15.3 ± 0.1

4 Conclusion

We have performed a systematic analysis of the isoscalar giant monopole resonance excitation energies in a wide spectrum of nuclei within the microscopic self-consistent Skyrme HF+BCS method with Skyrme SLy4 interaction and pairing correlations, as well as the coherent density fluctuation model. The method of calculations includes three steps. The first one is to determine the incompressibility of infinite nuclear matter $K(\rho_0(x))$. For this purpose, for the potentia part of the EDF we use that one of the Brueckner EDF and the one from the EDF of Barcelona-Catania-Paris-Madrid [BCPM(v)]. The second step includes calculations of the necessary incompressibility of finite nuclei within the CDFM scheme averaging the incompressibility of nuclear matter by the weight function $|F(x)|^2$ [Eq. (13)] that is related to the nucleon density distribution [Eq. (11)]. The CDFM allows one to obtain the quantities of finite nuclei (such as the symmetry energy, the incompressibility and others) on the base of the corresponding ones for nuclear matter. As a third step, we perform calculations of the centroid energies of the ISGMR based on the two definitions: the one that uses the radial parameter of the density distributions [Eq. (1)] and the other, in which the excitation energy is expressed through the mean square mass radius of the nucleus in the ground state [Eq. (2)]. The nuclear incompressibility K^A in both cases is calculated by using Eq. (13).

The results for the centroid energy deduced from Eq. (2) in the case of the Brueckner EDF are in good agreement with the data for the lighter isotopes of Ca, Fe, and Ni and acceptable for those of Zn, Mo, and Cd. In the case of BCMP(v) EDF they are comparable for some Pb isotopes and, in particular, for ^{68}Ni nucleus. The excitation energy of ISGMR in ^{68}Ni is located at higher energy (21.1 MeV) for the Ni isotopic chain due to the large fragmentation of the isoscalar monopole strength [3, 4]. Nevertheless, our value of 21.74 MeV reproduces very well the experimental one.

We have analyzed the problems related to the neutron density distributions which cannot be precisely obtained in many cases, as well as the corresponding rms radii. This point is of particular importance for the neutron-rich nuclei, which are the majority of the nuclei considered. Along this line, we preformed calculations of the ISGMR energy in cases when data for the neutron skin thickness are available. By using Eq. (2) we found that the results for the Sn isotopic chain (A=112-124), as well as for the double-magic ^{48}Ca and ^{208}Pb nuclei recently explored in CREX and PREX experiments, are almost insensitive regarding the extracted mean square mass radius to get values of the centroid energy.

By parametrization of the mass dependence of the radial parameter in the range between ^{40}Ca and ^{208}Pb nuclei, we have applied Eq. (1) to calculate the ISGMR energies. A good overall agreement with the experimental data for all considered nuclei is achieved when using the BCPM(v) functional. In conclusion, we would like to note that due the the lack of precise data for the neutron (and matter) rms radii the use of Eq. (1) is more preferable in the theoretical

calculations. In addition, we have noted that the comparison of the results for E_{ISGMR} using Eq. (1) and both EDFs of Brueckner and BCMP(v) shows the advantage of the second one. Finally, we note that new data and refined theoretical methods are necessary for the correct description of the breathing modes in medium-heavy nuclei, more specifically the placement of the ISGMR centroid energy.

References

[1] C. Monrozeau *et al.*, *Phys. Rev. Lett.* **100** (2008) 042501.

[2] S. Bagchi *et al.*, *Phys. Lett. B* **751** (2015) 371.

[3] M. Vandebrouck *et al.*, *Phys. Rev. Lett.* **113** (2014) 032504.

[4] M. Vandebrouck *et al.*, *Phys. Rev. C* **92** (2015) 024316.

[5] M.K. Gaidarov, M.V. Ivanov, Y.I. Katsarov, A.N. Antonov, *Astronomy* **2** (2023) 1.

[6] M.K. Gaidarov, M.V. Ivanov, Y.I. Katsarov, A.N. Antonov, I.C. Danchev, *Phys. Rev. C* **111** (2025) 064311.

[7] K.A. Brueckner, J.R. Buchler, S. Jorna, R. J. Lombard, *Phys. Rev.* **171** (1968) 1188.

[8] K.A. Brueckner, J.R. Buchler, R.C. Clark, R.J. Lombard, *Phys. Rev.* **181** (1969) 1543.

[9] M. Baldo, L.M. Robledo, X. Viñas, *Eur. Phys. J. A* **59** (2023) 156.

[10] M. Baldo, L.M. Robledo, P. Schuck, X. Viñas, *Phys. Rev. C* **87** (2013) 064305.

[11] M. Baldo, L.M. Robledo, P. Schuck, X. Viñas, *Phys. Rev. C* **95** (2017) 014318.

[12] A.N. Antonov, V.A. Nikolaev, I.Zh. Petkov, *Bulg. J. Phys.* **6** (1979) 151; *Z. Phys. A* **297** (1980) 257; *ibid* **304** (1982) 239; *Nuovo Cimento A* **86** (1985) 23; *Bulg. J. Phys.* **18** (1991) 107; A.N. Antonov *et al.*, *ibid* **102** (1989) 1701; A.N. Antonov, D.N. Kadrev, and P.E. Hodgson, *Phys. Rev. C* **50** (1994) 164.

[13] A.N. Antonov, P.E. Hodgson, I.Zh. Petkov, *Nucleon Momentum and Density Distributions in Nuclei* (Clarendon Press, Oxford, 1988); *Nucleon Correlations in Nuclei* (Springer-Verlag, Berlin-Heidelberg-New York, 1993).

[14] J.J. Griffin, J.A. Wheeler, *Phys. Rev.* **108** (1957) 311.

[15] K.A. Brueckner, M.J. Giannoni, R.J. Lombard, *Phys. Lett. B* **31** (1970) 97.

[16] S. Stringari, *Phys. Lett. B* **108** (1982) 232.

[17] M.K. Gaidarov, A.N. Antonov, P. Sarriguren, E. Moya de Guerra, *Phys. Rev. C* **84** (2011) 034316.

[18] H. De Vries, C.W. De Jager, C. De Vries, *At. Data Nucl. Data Tables* **36** (1987) 495.

[19] P. Sarriguren, M.K. Gaidarov, E. Moya de Guerra, A.N. Antonov, *Phys. Rev. C* **76** (2007) 044322.

[20] J.D. Patterson, R.J. Peterson, *Nucl. Phys. A* **717** (2003) 235.

[21] Li-Gang Cao, H. Sagawa, G. Colò, *Phys. Rev. C* **86** (2012) 054313.

[22] D. Adhikari *et al.*, *Phys. Rev. Lett.* **126** (2021) 172502.

[23] The CREX Collaboration, *Phys. Rev. Lett.* **129** (2022) 042501.

[24] R. Machleidt, F. Sammarruca, *Progr. Part. Nucl. Phys.* **137** (2024) 104117.